Stable polymer electrolytes based on polyether-grafted ZnO nanoparticles for all-solid-state lithium batteries

Huan-Ming Xiong, Zi-Dong Wang, Dong-Ping Xie, Liang Cheng and Yong-Yao Xia*

Received 10th October 2005, Accepted 5th January 2006
First published as an Advance Article on the web 20th January 2006
DOI: 10.1039/b514346b

Solid polymer nanocomposite electrolytes composed of polyethylene oxide (PEO) macromolecules, $LiN(CF_3SO_2)_2$ (LiTFSI) and polyether-grafted nano-ZnO (designated ZnO(PEGME)), are prepared and characterized in comparison with the prototypical PEO–LiTFSI film and that doped with conventional acetate group modified ZnO nanoparticles (designated ZnO(Ac)). High resolution transmission electron microscopic (HRTEM) results show that ZnO nanoparticles are dispersed homogeneously in the present PEO–LiTFSI–ZnO(PEGME) films, while those particles in PEO–LiTFSI–ZnO(Ac) aggregate badly. Atomic force microscopic (AFM) analyses prove that after storage at room temperature for a month, PEO–LiTFSI forms large dendrites while only a small amount of tiny crystals can be observed in the PEO–LiTFSI–ZnO(PEGME) film. In contrast, ZnO(Ac) particles agglomerate around the PEO–LiTFSI dendrites and separate from the original phase. This is the first direct observation on the micromorphology of the SPE films after long-term storage, which elucidates why the PEO–LiTFSI–ZnO(PEGME) electrolyte is much more stable than its counterparts. Conductivity evolutions, Li^+ transport number measurements and cycle performances of the above-mentioned three typical films in all-solid-state lithium batteries also suggest that the structural merits of the polyether-grafted nanoparticles render this type of SPEs attractive in the future applications.

Introduction

Solid polymer electrolytes (SPEs), because of their potential applications in all-solid-state lithium batteries, super capacitors and dye-sensitized solar cells, have attracted wide investigation in the past 30 years.[1–5] However, the prototypical SPE, a solid solution composed of some salts and PEO with high molecular weight, only exhibits 10^{-8}–10^{-7} S cm^{-1} conductivities at room temperature. To obtain SPEs with improved conductivities, many strategies have been suggested which include incorporating organic solvents,[6] doping inorganic fillers,[7] synthesizing new polymers or salts,[8] and preparing various organic–inorganic hybrids.[9] Among them, doping nano-oxides was regarded as the most promising method because the as-prepared SPEs have moderate ionic conductivities, enhanced mechanical properties and better electrochemical stabilities.[10] The positive effects of the nano-fillers arise from Lewis acid–base interactions[11] or dipole–dipole interactions[12] between nanoparticles and polymer electrolytes which suppress the crystallization of the polymer electrolytes and promote the disassociation of the ion pairs so that the electrolytes can release more free carriers and remain amorphous state for charge carriers to transfer. However, these interactions critically depend on the surface area and surface state of the nano-fillers. Since nanoparticles aggregate and grow spontaneously even in a solid matrix, their total surface area will decrease and their surface atoms will self-arrange to reduce surface vacancies which result in the loss of Lewis acidic/basic sites or dipoles, and thus both of the interactions become weaker and weaker during storage.[13] As a result, such nanoparticle-doped SPEs are mesostable and their improved properties usually decay along with time,[14] especially at higher temperatures,[15] and their properties critically depend upon their thermal history.[16] Actually, the direct observation on the micromorphologies of the composite SPE films after a long time of storage has not been reported yet. Furthermore, very few studies have been devoted to measuring the cycle performances of a polymer nanocomposite electrolyte in a real lithium battery where the SPE film works as an electrolyte and separator between a cathode and a lithium anode.[17]

In order to overcome the drawbacks of the nanoparticle-doped SPEs, we have succeeded in preparing a new type of SPEs which consist of polyether-grafted nano-oxides and lithium salts dissolved by these polyether groups.[18] Such SPEs have amorphous conductive layers (over 10^{-4} S cm^{-1} at room temperature) around the nano-oxide cores, and these nano-cores are prevented from aggregation by the outside polymer groups. These SPEs are very stable during storage and show no dependence upon thermal treatments because the surface PEO groups are connected with the nano-cores through covalent bonds and these PEO oligomers will not crystallize at room temperature. In this study, we prepared the conventional ZnO nanoparticles with Lewis basic sites (acetate groups) and polyether-grafted ZnO nanoparticles, and incorporated them into the prototypical PEO–LiTFSI films respectively. The conductivity evolutions of the composite films and their cycle performances in all-solid-state lithium batteries were compared. The results showed that the SPE films containing

Department of Chemistry, and Shanghai Key Laboratory of Molecular Catalysis and Innovative Materials, Fudan University, Shanghai 200433, People's Republic of China. E-mail: yyxia@fudan.edu.cn; Fax: (+86) 21 55664177

polyether-grafted ZnO nanoparticles had much better properties than their counterparts, as predicted by the micromorphology analyses.

Experimental

The ethanol solutions of ZnO(PEGME)[19] (PEGME is poly(ethylene glycol) methyl ether with molecular weight of 350, Aldrich) and ZnO(Ac)[20] were prepared according to our previous papers. LiTFSI (Aldrich) and PEO (MW = 4 000 000 g mol^{-1}, Aldrich) were dissolved in acetonitrile. The thermogravimetric analyses showed that there were about 40 wt% and 70 wt% ZnO contents for ZnO(PEGME)[18] and ZnO(Ac)[21] respectively. To prepare SPE films with the same amount of ZnO nanoparticles, the LiTFSI solution, PEO solution and ZnO colloids were mixed by appropriate ratios and dried to produce two typical SPE films in PTFE containers. One is PEO–LiTFSI–ZnO(PEGME) which has 20 wt% LiTFSI and 18 wt% ZnO(PEGME), the other is PEO–LiTFSI–ZnO(Ac) which contains 20 wt% LiTFSI and 10 wt% ZnO(Ac). For HRTEM measurements on a Jeol JEM-2010 transmission electron microscope operated at 200 kV, the diluted solutions of PEO–LiTFSI–ZnO(PEGME) and PEO–LiTFSI–ZnO(Ac) were dropped onto copper meshes respectively and dried. For AFM measurements on a Molecular Imaging Picoscan 2100 scanning probe microscope using a tapping mode,[22] the diluted solutions were dropped onto silicon substrates and kept in vacuum for a month before test. For electrical measurements using a Solartron SI 1287 electrochemical interface and a Solartron SI 1250 impedance/gain-phase analyzer, the concentrated solutions were dried in PTFE containers under vacuum to form films with thickness of about 300 μm. The films were sandwiched between two stainless steel electrodes to test the AC impedance spectra and between two lithium electrodes to evaluate Li^+ transport numbers through the classical steady-state-current method.[23] In order to compare the performances of the SPE films in all-solid-state lithium batteries, $Li_{0.33}MnO_2$ was synthesized[24] and mixed (65 wt%) with active carbon (5 wt%) and PEG–LiTFSI (30 wt%, PEG is polyethylene glycol with molecular weight of 2000 g mol^{-1}, molar ratio [EO]/[Li] = 20). In an argon filled glove box, the mixture was ground thoroughly, melted at 100 °C and then cast on a piece of aluminium foil as the cathode. The PEO–LiTFSI–ZnO(PEGME), PEO–LiTFSI–ZnO(Ac) and PEO–LiTFSI films were sandwiched between the cathode materials and lithium flakes as anodes to assemble CR2016 coin-type cells. These $Li_{0.33}MnO_2$/SPE/Li cells were cycled within 2.0–3.4 V at 60 °C at a current density of 0.1 mA cm^{-2}.

Results and discussion

In Fig. 1, the HRTEM photos of the as-prepared PEO–LiTFSI–ZnO(PEGME) and PEO–LiTFSI–ZnO(Ac) films are shown. Although the ZnO nanoparticles are not very clear due to the electron absorption/reflection by polymers, it is obvious that ZnO(PEGME) nanoparticles are dispersed homogeneously in the SPE film while the ZnO(Ac) nanoparticles aggregated heavily. This distinction is ascribed to the difference of the surface groups on ZnO nanoparticles, because

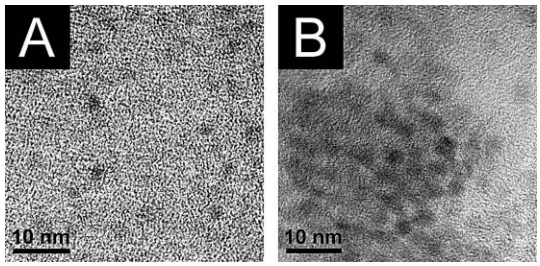

Fig. 1 HRTEM photographs of the (A) PEO–LiTFSI–ZnO(PEGME) film and (B) PEO–LiTFSI–ZnO(Ac) film.

the diameters of ZnO nanoparticles for both samples are controlled to be about 3 nm. ZnO(PEGME) nanoparticles dissolve in PEO to form a solid solution, but the ZnO(Ac) nanoparticles agglomerate and separate from the PEO–LiTFSI phase when the solvents evaporate. After the samples are stored in vacuum at room temperature for a month, the AFM topograph and amplitude images of the PEO–LiTFSI, PEO–LiTFSI–ZnO(PEGME) and PEO–LiTFSI–ZnO(Ac) films are taken and shown in Fig. 2. The PEO–LiTFSI (sample A) exhibits typical dendrites with feature heights of about 100 nm while the crystalline regions in PEO–LiTFSI–ZnO(PEGME) film (sample B) are tiny and irregular, with their feature heights less than 10 nm, indicating that the ZnO(PEGME) nanoparticles suppress the PEO–LiTFSI crystallization effectively. Furthermore, ZnO(PEGME) nanoparticles can not be detected because they have dissolved in the PEO–LiTFSI film to form a uniform phase. In contrast, Fig. 2C shows that ZnO(Ac) aggregate around the PEO–LiTFSI dendrites to form arborization patterns. It has been regarded for many years that in the nanoparticle-doped SPEs the nano-fillers were dispersed homogeneously and PEO macromolecules prevented them from agglomeration.[25,26] However, our AFM results directly illustrate that after storage for weeks the PEO–LiTFSI–ZnO(Ac) are crystalline and multiphase, which is a convincing proof for the property decay of the nanoparticle-doped SPEs. And the PEO-based SPEs containing other nano-oxides behave similarly as was expected.

It is the composition, structure and morphology that determine the property and performance of the SPE film. In Fig. 3, the conductivity evolutions of three typical SPE films during storage at room temperature are compared. It is seen that all samples exhibit stable conductivities after storage for about 20 days. Although the ZnO(Ac) doped films (sample b) have enhanced conductivity than the prototypical one (sample a), the PEO–LiTFSI–ZnO(PEGME) film (sample c) exhibit much higher conductivity that is above 10^{-5} S cm^{-1} at 20 °C. The conductivity changes of these samples are also recorded during heating scans, as shown in Fig. 4. The curve for the prototypical PEO–LiTFSI (sample e) exhibits a turning point at about 70 °C where the crystalline phase in sample e melts. Both the freshly prepared PEO–LiTFSI–ZnO(PEGME) film (sample a) and PEO–LiTFSI–ZnO(Ac) film (sample c) are wholly amorphous, but after storage at room temperature for a month, the PEO–LiTFSI–ZnO(Ac) film (sample d) has crystallized heavily while the PEO–LiTFSI–ZnO(PEGME) (sample b) keeps amorphous and shows only a slight decrease

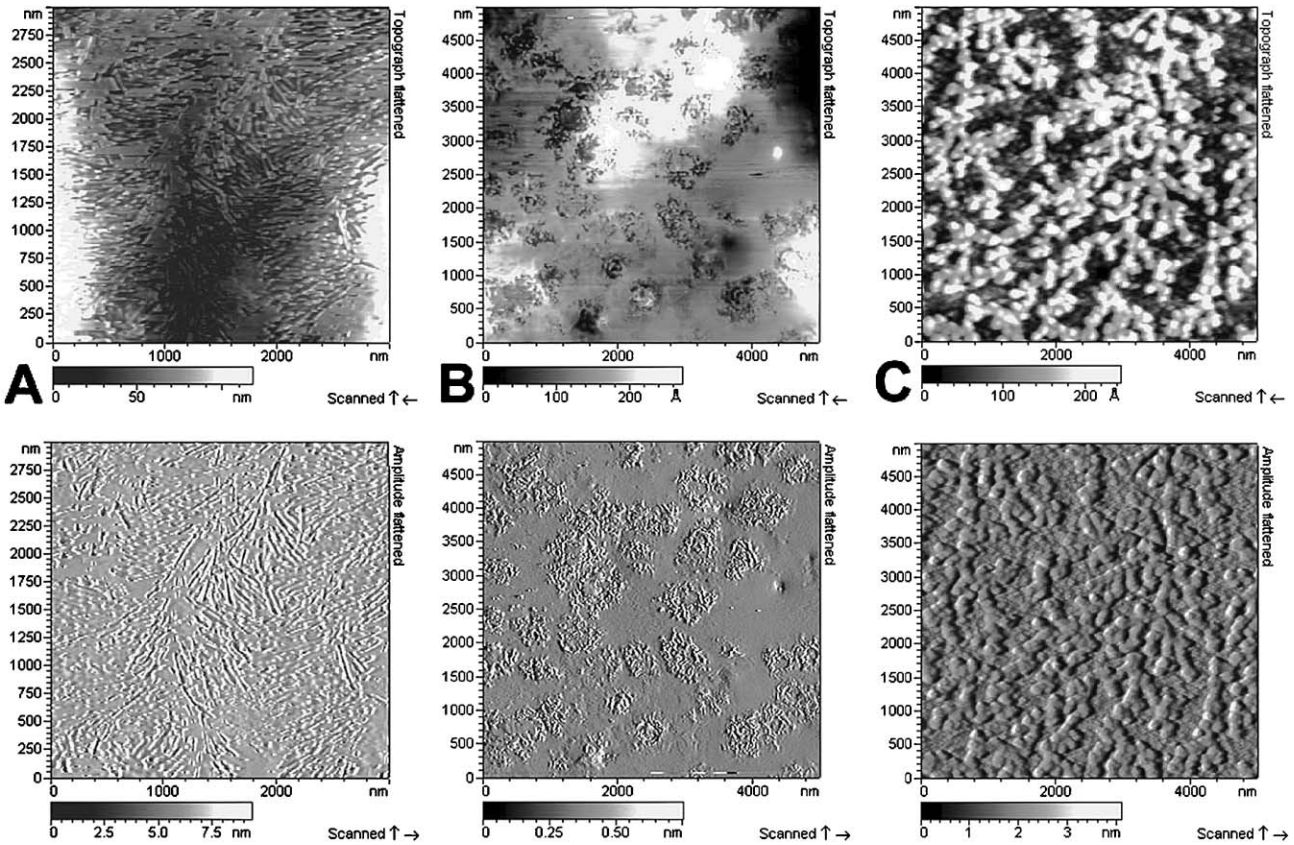

Fig. 2 Topograph (upper) and amplitude (nether) images of the SPE films on silicon substrates obtained by a tapping mode AFM measurement. (A) PEO–LiTFSI, (B) PEO–LiTFSI–ZnO(PEGME) and (C) PEO–LiTFSI–ZnO(Ac) are kept in vacuum at room temperature for a month before test.

in conductivity. Here, at least two methods were used to determine the SPE crystalline. One is observing by AFM, the other is heating scans. If the sample is amorphous, the corresponding heating curve will not exhibit a turning point when the crystalline phase melts. To avoid the influence of the PEO–LiTFSI crystallization on the Li^+ transport numbers of

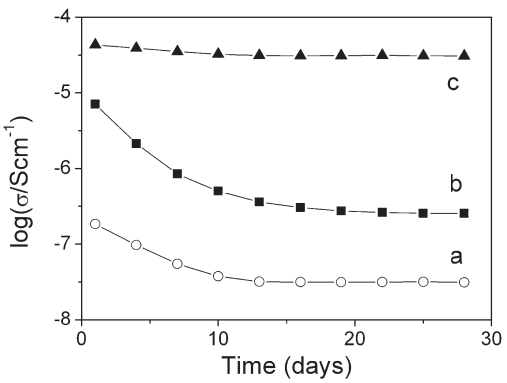

Fig. 3 Conductivity evolution of the SPE films during storage at room temperature. Samples (a) PEO–LiTFSI, (b) PEO–LiTFSI–ZnO(Ac) and (c) PEO–LiTFSI–ZnO(PEGME) are sandwiched between two stainless steel electrodes and kept in an argon filled glove box at room temperature.

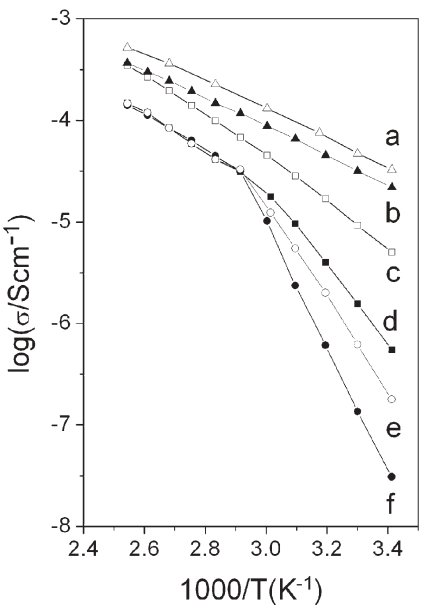

Fig. 4 Conductivities of different samples in the heating scan. These SPEs consist of PEO and 20 wt% $LiN(CF_3SO_2)_2$ with (a) 18 wt% ZnO(PEGME), (c) 10 wt% ZnO(Ac) and (e) no fillers respectively. Samples b, d and f are obtained by keeping samples a, c and e in vacuum at room temperature for a month respectively.

the samples, three typical films were kept at 60 °C for 24 h, and then measured using the classical steady-state-current method in which 10 mV was applied on the Li/SPE/Li cells until the direct current reached a stable value. The calculated results were 0.20–0.25, 0.35–0.40 and 0.45–0.55 for the PEO–LiTFSI, PEO–LiTFSI–ZnO(Ac) and PEO–LiTFSI–ZnO(PEGME) films respectively, but these results have considerable errors due to the method itself.[27]

The differences in the conductivities and transport numbers between PEO–LiTFSI–ZnO(PEGME) (sample A) and PEO–LiTFSI–ZnO(Ac) (sample B) can be explained by Scheme 1. In both samples, the black balls represent ZnO nanoparticles, the grey regions are the crystalline PEO–LiTFSI and the white regions are the highly conductive amorphous layers around ZnO nanoparticles. For sample A, the white regions consist of LiTFSI and naturally amorphous PEGME oligomers, while for sample B, the amorphous regions, which are mesostable, result from some interactions between ZnO(Ac) and PEO–LiTFSI. Since the ZnO(PEGME) nanoparticles are dissolved in the solid phase, the white regions are continuous and the carriers can transfer easily. On the contrary, the amorphous regions are discontinuous in sample B because the ZnO(Ac) nanoparticles can not dissolve in the PEO–LiTFSI phase and the ZnO(Ac) aggregates are separated from each other. Therefore, the conductivity and transport number of sample B are definitely lower than those for sample A.

The essential properties for practical SPEs are their performances when they are assembled into a real device and tested by cycles. In this study, $Li_{0.33}MnO_2$ is employed as the active material for the cathode because such a cell works properly under 3.5 V, and thus the decomposition of PEO on active carbon surface during charging process is avoided thoroughly. It should be mentioned that decomposition voltage obtained from typical electrochemical window measurements is not in accord with the data obtained under the practical conditions in a lithium battery. For example, PEO-base SPEs usually exhibit electrochemical windows above 5 V when the films are sandwiched between lithium electrodes or inert electrodes and scanned slowly by voltammetry method, but they often decompose on the active carbon surfaces below 4 V in an all-solid-state lithium cell.[17] Hence, a suitable cathode is crucial for a lithium cell employing SPE and lithium anode.[24] Another important factor is the impedance and Li^+ transport number of the SPEs, which determines how much capacity the cell can release. The impedance of the SPE films depends on the conductivity and the thickness of the films. However, we can only prepare films thicker than 300 μm by now, because thinner films are difficult to handle in a glove box and their mechanical strength is not sufficient for assembly.

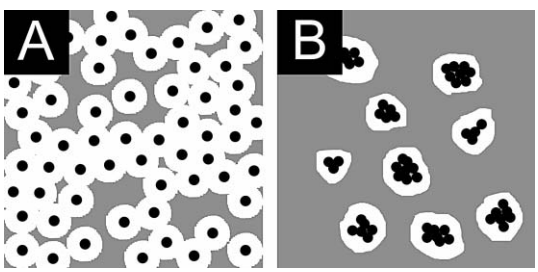

Scheme 1 Schematic diagrams of SPE films (A) PEO–LiTFSI–ZnO(PEGME) and (B) PEO–LiTFSI–ZnO(Ac).

In Fig. 5, the performances of three typical SPE films in lithium batteries are compared. Although the PEO–LiTFSI film (sample A) exhibit the best cycle performance, its impedance is so large that the cell capacity is only about 43 mA h g^{-1}. With higher conductivity and transport number, our PEO–LiTFSI–ZnO(PEGME) makes the cell exhibit about 100 mA h g^{-1} capacity in the first 20 cycles. In comparison, the cell employing PEO–LiTFSI–ZnO(Ac) electrolyte is not stable, with its capacity decreasing rapidly from 62 mA h g^{-1} to 43 mA h g^{-1} during the initial three cycles, which suggests that the ZnO(Ac) nano-fillers aggregate slowly and lose their positive effects in the melted SPE system. Although the curves

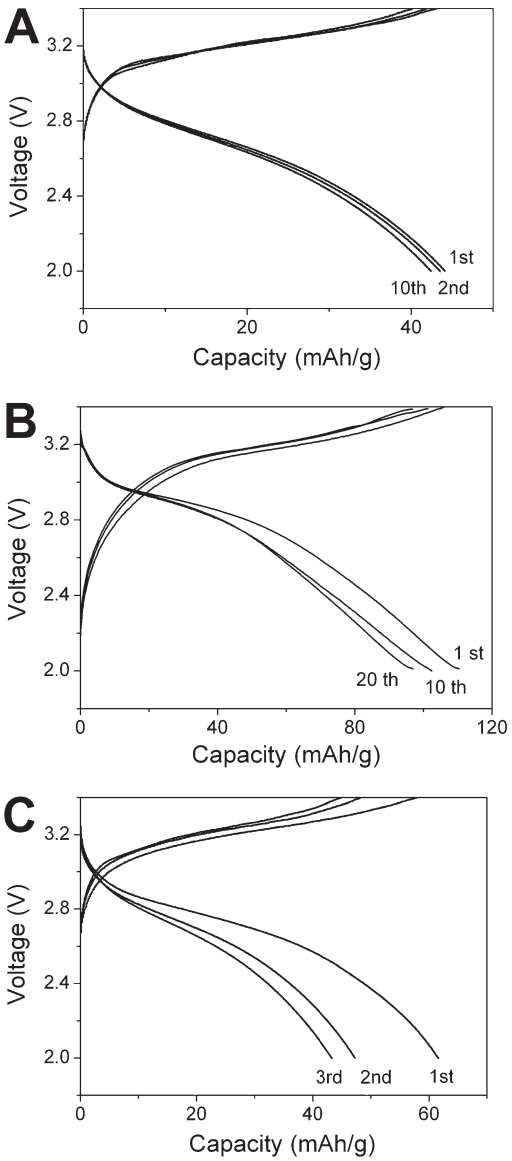

Fig. 5 Cycle performances of the SPEs films in $Li_{0.33}MnO_2$/SPE/Li cells at 60 °C. These films are (A) PEO–LiTFSI, (B) PEO–LiTFSI–ZnO(PEGME) and (C) PEO–LiTFSI–ZnO(Ac) with average thickness of about 300 μm.

for PEO–LiTFSI–ZnO(PEGME) film shows the largest capacity among the present SPEs, the released capacity is smaller than those reported by other researchers who found $Li_{0.33}MnO_2$ could delivered a capacity of more than 150 mA h g^{-1} when using SPE films with thickness of about 10 μm.[28] Hence, our further research is carried on to improve the film preparation techniques and the cell assembly processes.

Conclusion

Three typical solid polymer electrolyte films PEO–LiTFSI, PEO–LiTFSI–ZnO(Ac) and PEO–LiTFSI–ZnO(PEGME) were prepared and characterized respectively. Among them, PEO–LiTFSI–ZnO(PEGME) exhibited the best properties including conductivity, stability and capability in a real lithium battery. This result is ascribed to the structural merits of the polyether-grafted nanoparticles, in which lithium salts are dissolved by the short PEO chains to form amorphous conductive layers and nanoparticle cores are protected by the surface polymer groups. The long-term stability of this SPE results from the miscibility of ZnO(PEGME) nanoparticles with PEO macromolecules, and the covalent bonding between PEGME and ZnO which is much stronger than the Lewis acid/base interactions or dipole–dipole interactions in the traditional nanoparticle-doped SPEs. Our work pushes solid polymer nanocomposite electrolytes to step forward to practical applications in all-solid-state lithium batteries and other electrical devices.

Acknowledgements

This work was supported by National Natural Science Foundation of China (Grant No. 20373014, 20503007).

References

1 P. V. Wright, *Br. Polym. J.*, 1975, **7**, 319.
2 C. A. Angell, C. Liu and E. Sanchez, *Nature*, 1993, **362**, 137.
3 F. Croce, G. B. Appetecchi, L. Persi and B. Scrosati, *Nature*, 1998, **394**, 456.
4 Z. Gadjourova, Y. G. Andreev, D. P. Tunstall and P. G. Bruce, *Nature*, 2001, **412**, 520.
5 J.-M. Tarascon and M. Armand, *Nature*, 2001, **414**, 359.
6 A. G. Bishop, D. R. MacFarlance, D. McNaughton and M. Forsyth, *J. Phys. Chem.*, 1996, **11**, 2237.
7 W. Wieczorek, A. Zalewska, D. Raducha, Z. Florjańczyk and J. R. Stevens, *J. Phys. Chem. B*, 1998, **102**, 352.
8 W. H. Meyer, *Adv. Mater.*, 1998, **10**, 439.
9 R. Ulrich, J. W. Zwanziger, S. M. D. Paul, A. Reiche, H. Leuninger, H. W. Spiess and U. Wiesner, *Adv. Mater.*, 2002, **14**, 1134.
10 F. Croce, R. Curini, A. Martinelli, L. Persi, F. Ronci, B. Scrosati and R. Caminiti, *J. Phys. Chem. B*, 1999, **103**, 10632.
11 W. Wieczorek, P. Lipka, G. Żukowska and H. Wyciślik, *J. Phys. Chem. B*, 1998, **102**, 6968.
12 H. M. Xiong, J. S. Chen and D. M. Li, *J. Mater. Chem.*, 2003, **13**, 1994.
13 H. M. Xiong, D. P. Liu, H. Zhang and J. S. Chen, *J. Mater. Chem.*, 2004, **14**, 2775.
14 H. M. Xiong, K. K. Zhao, X. Zhao, Y. W. Wang and J. S. Chen, *Solid State Ionics*, 2003, **159**, 89.
15 B. Kumar, L. G. Scanlon and R. J. Spry, *J. Power Sources*, 2001, **96**, 337.
16 B. Kumar, S. J. Rodrigues and L. G. Scanlon, *J. Electrochem. Soc.*, 2001, **148**, A1191.
17 C. Wang, Y. Xia, K. Koumoto and T. Sakai, *J. Electrochem. Soc.*, 2002, **149**, A967.
18 H. M. Xiong, Z. D. Wang, D. P. Liu, J. S. Chen, Y. G. Wang and Y. Y. Xia, *Adv. Funct. Mater.*, 2005, **15**, 1751.
19 H. M. Xiong, D. P. Liu, Y. Y. Xia and J. S. Chen, *Chem. Mater.*, 2005, **17**, 3062.
20 H. M. Xiong, X. Zhao and J. S. Chen, *J. Phys. Chem. B*, 2001, **105**, 10169.
21 S. Sakohara, L. D. Tickanen and M. A. Anderson, *J. Phys. Chem.*, 1992, **96**, 11086.
22 Y. Gu, H. Xie, J. Gao, D. Liu, C. T. Williams, C. J. Murphy and H. J. Ploehn, *Langmuir*, 2005, **21**, 3122.
23 J. Evans, C. A. Vincent and P. G. Bruce, *Polymer*, 1987, **28**, 2334.
24 Y. Xia, K. Tatsumi, T. Fujieda, P. P. Prosini and T. Sakai, *J. Electrochem. Soc.*, 2000, **147**, 2050.
25 F. M. Gray, *Polymer Electrolytes*, The Royal Society of Chemistry, Cambridge, 1997, ch. 2, p. 53.
26 B. Kumar and L. G. Scanlon, *J. Power Sources*, 1994, **52**, 261.
27 L. Edman, M. M. Doeff, A. Ferry, J. Kerr and L. C. De Jonghe, *J. Phys. Chem. B*, 2000, **104**, 3476.
28 G. Jiang, S. Maeda, H. Yang, C. Wang, Y. Saito, S. Tanase and T. Sakai, *J. Electrochem. Soc.*, 2004, **151**, A1886.